Inorganic Chemistry

Article

pubs.acs.org/IC

Family of Mixed 3d–4f Dimeric 14-Metallacrown-5 Compounds: Syntheses, Structures, and Magnetic Properties

Fan Cao,[†,‡] Suna Wang,[†,‡] Dacheng Li,[†] Suyuan Zeng,[†] Meiju Niu,[†] You Song,*[,‡] and Jianmin Dou*[,†]

[†]Shandong Provincial Key Laboratory of Chemical Energy Storage and Novel Cell Technology, School of Chemistry and Chemical Engineering, Liaocheng University, 252059 Liaocheng, People's Republic of China

[‡]State Key Laboratory of Coordination Chemistry, Nanjing National Laboratory of Microstructures, School of Chemistry and Chemical Engineering, Nanjing University, 210093 Nanjing, People's Republic of China

Supporting Information

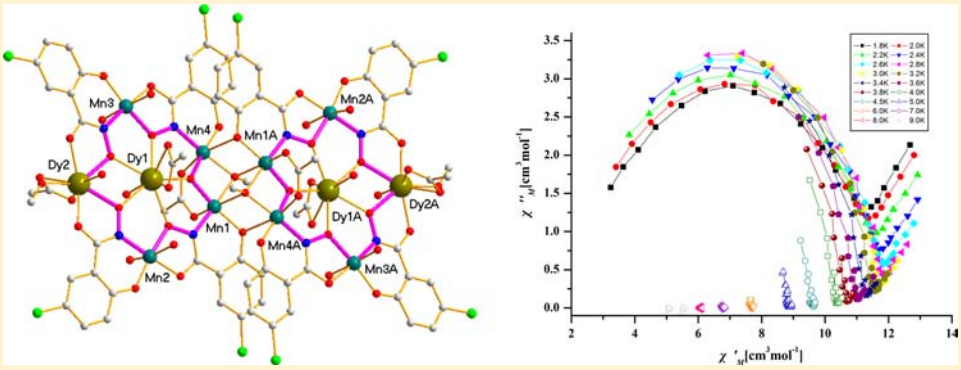

ABSTRACT: An isomorphous family of mixed 3d–4f dodenuclear aggregates, $\{[Mn^{III}_8Ln_4(Clshi)_8(OAc)_6(\mu_3\text{-}OCH_3)_2(\mu_3\text{-}O)_2(CH_3OH)_{12}(H_2O)_2]\cdot 4CH_3OH\cdot xH_2O\}$ (where Ln = Eu^{III} (**1**), Gd^{III} (**2**), Tb^{III} (**3**), and Dy^{III} (**4**); $ClshiH_3$ = 5-chlorosalicylhydroxamic acid; x = 5 for **1** and **3**; x = 6 for **2**; x = 2 for **4**), were synthesized and characterized. They were obtained from the reaction of $ClshiH_3$ with $Mn(OAc)_2\cdot 4H_2O$ and $Ln(NO_3)_3\cdot 6H_2O$. These isomorphous mixed 3d–4f compounds represent a family of novel structures with lanthanide ions in the metallacrown (MC) ring. Each dodecanuclear aggregate contains two offset stacked 14-MC-5 units with M–N–O–M–N–O–Ln–O–N–M–O–N–M connectivity to capture one Ln^{III} ion in the core of each MC. Two 14-MC-5 units are connected through O ions with four Mn ions and six O atoms arranged in a double Mn_4O_6 cubane. Magnetic measurement indicates that antiferromagnetic interactions are present between the metal ions. The Dy^{III} analogue with high anisotropy and large spin shows slow magnetization relaxation at a direct-current field of 2 kOe.

INTRODUCTION

Metallacrowns (MCs), a kind of metallamacrocycle compound similar to organic crowns with O or N atoms replaced by metal atoms, were reported in 1989, with the first structures represented by $[VO(shi)(MeOH)]_3$ (9-MC-3) and $Mn(OAc)_2[Mn_4(shi)_4(DMF)_6]\cdot 2DMF$ (12-MC-4; DMF = *N*,*N*-dimethylformamide and shi = salicylhydroxamic acid).[1] Since then, MCs have received much attention not only for their diverse architectures but also for their potential applications in host–guest recognition and bioactivities.[2,3] Considerable efforts have been devoted to magnetic studies of these kinds of compounds since the initial discovery of single-molecule magnets (SMM) in 1993.[4−7] The SMM behavior is strongly related with large ground-state spin [S] and large easy-axis anisotropy [negative zero-field-splitting (ZFS) parameter, D]. Structurally, MCs typically possess a large number of metal ions to provide a large spin. The configuration easily enforces a planar arrangement of the metal ions by controlling the topology of the compounds through alignment of single-ion magnetoanisotropy, and therefore a large molecular ZFS parameter (D) could be obtained. That is why MCs could potentially behave as SMMs.

The selection of suitable metal ions is important to SMMs. A high-spin Mn^{III} ion has four unpaired electrons per ion (S = 2) and large anisotropy because of its Jahn–Teller (JT) axis, which has been the most popular in the construction of SMMs. With both large spin and considerable single-ion anisotropy, a single anisotropic magnetic Ln^{III} ion in an axial crystal-field environment could provide sufficient conditions to establish a thermal barrier for reversal of the magnetization.[8] A combination of these two kinds of metal ions in one compound may lead to SMM behavior. Up to now, manganese–lanthanide (Mn–Ln) SMMs have also garnered considerable attention, such as $Mn–Gd_2$, $Mn_2–Gd$, $Mn_2–Ln_2$, $Mn_2–Dy_2$, $Mn_2–Ln_3$, $Mn_2–Ln_4$, $Mn_3–Ln$, $Mn_4–Ln_2$, $Mn_4–Ln_3$, $Mn_4–Ln_4$, $Mn_4–Gd_4$, $Mn_4–Dy_6$, $Mn_5–Ln_4$, $Mn_5–Tb_6$, $Mn_5–Ln_8$, $Mn_6–Ce_2$, $Mn_6–Ln_2$, $Mn_6–Ln_4$, $Mn_6–Dy_6$, $Mn_8–Ce$, $Mn_9–Dy_8$, $Mn_{10}–Ln_2$,

Received: November 27, 2012
Published: September 25, 2013

 © 2013 American Chemical Society dx.doi.org/10.1021/ic3025952 | *Inorg. Chem.* 2013, 52, 10747–10755

Table 1. Crystallographic Data and Structure Refinement for Compounds 1−4

	1	2	3	4
formula	$C_{86}H_{126}Cl_8Eu_4Mn_8N_8O_{63}$	$C_{86}H_{128}Cl_8Gd_4Mn_8N_8O_{64}$	$C_{86}H_{126}Cl_8\ Tb_4Mn_8N_8O_{63}$	$C_{86}H_{124}Cl_8Dy_4Mn_8N_8O_{62}$
M_r	3610.91	3650.08	3638.75	3635.05
cryst size [mm^3]	0.26 × 0.23 × 0.15	0.32 × 0.29 × 0.18	0.36 × 0.34 × 0.33	0.36 × 0.35 × 0.33
color	black	black	black	black
cryst syst	triclinic	triclinic	triclinic	triclinic
space group	$P\bar{1}$	$P\bar{1}$	$P\bar{1}$	$P\bar{1}$
T [K]	298(2)	298(2)	298(2)	298(2)
a [Å]	12.9509(11)	12.9985(11)	12.9208(7)	12.9550(11)
b [Å]	12.9702(12)	13.0134(12)	12.9568(8)	12.9788(12)
c [Å]	20.4300(18)	20.455(2)	20.2851(11)	20.3847(16)
V [Å^3]	3322.7(5)	3350.8(5)	3283.0(3)	3317.7(5)
Z	1	1	1	1
ρ_{calcd} [mg m^{-3}]	1.745	1.803	1.843	1.721
λ [Å]	0.71073	0.71073	0.71073	0.71073
μ [mm^{-1}]	2.838	2.927	3.122	3.202
F(000)	1718	1792	1796	1680
reflns collected/unique reflns	16111/11506	16867/11638	22006/11576	16482/11425
R_{int}	0.0334	0.0413	0.0435	0.0259
GOF on F^2	1.063	1.047	1.052	1.144
R1 [$I > 2\sigma(I)$], wR2 (all data)	0.0475, 0.1402	0.0530, 0.1612	0.0525, 0.1428	0.0546, 0.1777

Mn_{11}−Ln_4, Mn_{11}−Gd_2, Mn_{12}−Gd_2, Mn_{12}−Dy_6, Mn_{12}−Ce_{22}, Mn_{18}−Dy, and Mn_{21}−Dy.[9−20]

In 2010, Pecoraro et al. first incorporated a Ln^{III} ion into the MC ring and reported mixed 3d−4f Mn_4−Ln_2-14-MC-5 compounds, namely, $[Ln_2Mn_4O(OH)(OAc)(NO_3)_2(shi)_4]\cdot 3C_3H_7NO\cdot 7C_5H_5N\cdot H_2O$ (Ln = Y, Gd, Tb, Dy, and Ho), among which Tb-14-MC-5, Dy-14-MC-5, and Ho-14-MC-5 showed slow magnetic relaxation, with Dy-14-MC-5 demonstrating a blocking temperature above 2 K.[10d] The authors reported that uniaxial anisotropy was a critical factor to maximize the overall anisotropy of a compound and the utility of the planar MC structure aligning the easy axes parallel to each other should be extended in order to create an SMM. The Dy^{III} analogue showed the highest blocking temperature, suggesting that Dy^{III} may have the highest "blend" of spin and anisotropy needed for effective SMMs. It was also confirmed by a planar Mn-12-MC-4 involving a Mn^{II} ion in the center cavity of the MC ring.[21] Otherwise, geometric control of the metal center in the cavity of the MC ring has proven to be an efficient path to maximizing the single-ion magnetoanisotropy in the Mn_5-12-MC-4 compound.

We have also focused on MC chemistry and recently reported a novel 9-MC-3 and 15-MC-6 onset stacked MC SMM, $[Mn_9O_4(Me\text{-}sao)_6(MeO)_3(O_2CMe)_3(OH)(MeOH)_2]\cdot 2.5DMF$ (Me-saoH$_2$ = 2-hydroxyphenylethanone oxime).[22,23] Herein, we report the syntheses and characterization of $\{Mn_4$−$Ln_2\}_2$ dimeric 14-MC-5 compounds assembled from 5-chlorosalicylhydroxamic acid, $\{[Mn^{III}{}_8Ln_4(Clshi)_8(OAc)_6(\mu_3\text{-}OCH_3)_2(\mu_3\text{-}O)_2(CH_3OH)_{12}(H_2O)_2]\cdot 4CH_3OH\cdot xH_2O\}$ (where Ln = Eu^{III} (**1**), Gd^{III} (**2**), Tb^{III} (**3**), and Dy^{III} (**4**); x = 5 for **1** and **3**; x = 6 for **2**; x = 2 for **4**). The isomorphous compounds represent a family of novel mixed 3d−4f compounds with lanthanide in the MC ring. Each structure consists of two offset stacked monomer 14-MC-5 units with M−N−O−M−N−O−Ln−O−N−M−O−N−M connectivity to capture one Ln^{III} ion in the core of each MC, similar to the reported examples by Pecoraro's group. Two μ_3-CH_3O^- groups and two η^2-O atoms of different 5-$Clshi^{3-}$ ligands bridge two 14-MC-5 units with four Mn ions and six O atoms in a double Mn_4O_6 cubane arrangement, forming a novel dimeric 14-MC-5 structure. Magnetic measurement indicates that antiferromagnetic interactions are dominant between the metal ions. The Dy^{III} analogue with high anisotropy and large spin shows slow magnetization relaxation at a direct-current (dc) field of 2 kOe. The different structures and magnetic properties between these dimeric 14-MC-5 compounds and similar monomer 14-MC-5 compounds were discussed in detail.

EXPERIMENTAL SECTION

Materials and Syntheses. All reagents were obtained from commercial sources and were used as received, without further purification. All reactions were carried out under aerobic conditions. 5-Chlorosalicylhydroxamic acid (ClshiH$_3$) was prepared by the condensation of 5-chlorosalicylic acid and hydroxylamine in a 1:1 molar ratio in water according to a modified procedure reported previously.[24]

Synthesis of $[Mn^{III}{}_8Eu^{III}{}_4(Clshi)_8(OAc)_6(\mu_3\text{-}OCH_3)_2(\mu_3\text{-}O)_2(CH_3OH)_{12}(H_2O)_2]\cdot 4CH_3OH\cdot 5H_2O$ (1). $Eu(NO_3)_3\cdot 6H_2O$ (0.338 g, 1 mmol) was added to a stirred solution of $Mn(OAc)_2\cdot 4H_2O$ (0.980 g, 4 mmol) and ClshiH$_3$ (0.752 g, 4 mmol) in MeOH (25 mL), and the pH was adjusted to 8 with $[(C_4H_9)_4N]OH$. The solution immediately became green and was stirred at room temperature. After 6 h, the color changed to dark green, and then the solution was filtered and left undisturbed at room temperature. The black block single crystals, suitable for X-ray diffraction analysis, were obtained after 2 weeks. These crystals were collected by filtration, washed with cold MeOH, and dried in air. Yield: 13 mg (27%, based on the ligand). Elem anal. Calcd for $C_{86}H_{126}Cl_8Eu_4Mn_8N_8O_{63}$: C, 28.58; H, 3.52; N, 3.10. Found: C, 28.19; H, 3.61; N, 3.22. IR (KBr, cm^{-1}): 3234(vs), 2867(s), 2687(w), 1231(m), 1235(w), 1879(m), 1235(s), 1679(w), 1145(m), 1689(m), 925(m), 748(m), 669(m), 612(m), 578(m).

Synthesis of $[Mn^{III}{}_8Gd^{III}{}_4(Clshi)_8(OAc)_6(\mu_3\text{-}OCH_3)_2(\mu_3\text{-}O)_2(CH_3OH)_{12}(H_2O)_2]\cdot 4CH_3OH\cdot 6H_2O$ (2). This compound was obtained as brown block crystals according to the procedure for **1**, using $Gd(NO_3)_3\cdot 6H_2O$ (0.343 g, 1 mmol) in place of $Eu(NO_3)_3\cdot 6H_2O$. Yield: 17 mg (31%, based on the ligand). Elem anal. Calcd for $C_{86}H_{128}Cl_8Gd_4Mn_8N_8O_{64}$: C, 28.30; H, 3.53; N, 3.07. Found: C, 27.97; H, 3.64; N, 3.37. IR (KBr, cm^{-1}): 2969(w), 1654(s), 1765(s), 1876(m), 1453(m), 1786(m), 1564(s), 1254(m), 1687(m), 1235(w), 968(w), 856(w), 778(m), 668(m), 594(m), 457(w), 423(m).

Synthesis of $[Mn^{III}{}_8Tb^{III}{}_4(Clshi)_8(OAc)_6(\mu_3\text{-}OCH_3)_2(\mu_3\text{-}O)_2(CH_3OH)_{12}(H_2O)_2]\cdot 4CH_3OH\cdot 5H_2O$ (3). This compound was obtained as brown block crystals according to the procedure for **1**,

dx.doi.org/10.1021/ic3025952 | Inorg. Chem. 2013, 52, 10747−10755

Table 2. Selected Bond Distances (Å) and Angles (deg) for Compounds 1−4[a]

1				**3**			
Eu1−O3	2.467(5)	Mn1−O14	1.967(5)	Tb1−O3	2.456(6)	Mn1−O22	2.195(6)
Eu1−O6	2.367(5)	Mn1−O26	2.197(6)	Tb1−O6	2.363(6)	Mn1−O39	1.866(6)
Eu1−O13	2.279(5)	Mn1−N1	1.956(7)	Tb1−O31	2.434(7)	Mn1−N1	1.957(7)
Eu1−O24	2.484(6)	Mn2−O2	1.912(5)	Tb1−O39	2.255(5)	Mn2−O2	1.912(6)
Eu2−O5	2.305(6)	Mn2−O3	1.931(5)	Tb2−O5	2.304(6)	Mn2−O3	1.929(5)
Eu2−O6	2.350(5)	Mn2−O4	1.857(6)	Tb2−O6	2.326(6)	Mn2−O4	1.865(6)
Eu2−O15	2.411(6)	Mn2−O18	2.325(6)	Tb2−O14	2.384(6)	Mn2−O17	2.322(6)
Eu2−O20	2.442(7)	Mn2−O23	2.241(7)	Tb2−O18	2.407(7)	Mn2−O25	2.250(6)
Mn1−O1	1.849(5)	Mn2−N2	1.923(7)	Mn1−O1	1.859(6)	Mn2−N2	1.926(7)
Mn1−O13	1.872(5)			Mn1−O13	2.529(6)		
Eu1−O6−Eu2	111.8(2)	Eu1−O13−Mn4	130.8(2)	Tb1−O6−Tb2	111.8(2)	Tb2−O39−Mn4	130.5(3)
Eu1−O13−Mn1	129.2(2)	Mn1−O13−Mn4	98.3(2)	Tb2−O39−Mn1	130.4(3)	Mn1−O39−Mn4	97.8(2)
Eu1−O3−Mn2	123.8(2)	Mn1−O14−Mn4A	105.7(2)	Tb2−O3−Mn2	123.8(3)	Mn1−O13−Mn4A	105.2(2)
Eu1−O12−Mn3	123.7(2)	Mn4−O14−Mn4A	102.3(2)	Tb2−O12−Mn3	123.8(2)	Mn4−O13−Mn4A	102.4(2)
2				**4**			
Gd1−O3	2.458(6)	Mn1−O14	1.975(6)	Dy1−O3	2.450(6)	Mn1−O28	1.965(6)
Gd1−O6	2.363(6)	Mn1−O27	2.208(7)	Dy1−O6	2.353(6)	Mn1−O31	1.864(6)
Gd1−O13	2.301(6)	Mn1−N1	1.965(8)	Dy1−O18	2.425(7)	Mn1−N1	1.965(7)
Gd1−O24	2.456(8)	Mn2−O2	1.919(7)	Dy1−O31	2.260(6)	Mn2−O2	1.917(7)
Gd2−O5	2.308(7)	Mn2−O3	1.935(6)	Dy2−O5	2.280(7)	Mn2−O3	1.942(6)
Gd2−O6	2.340(6)	Mn2−O4	1.862(7)	Dy2−O6	2.310(7)	Mn2−O4	1.874(7)
Gd2−O15	2.405(7)	Mn2−O18	2.319(8)	Dy2−O15	2.375(9)	Mn2−O16	2.324(7)
Gd2−O20	2.431(9)	Mn2−O25	2.254(8)	Dy2−O29	2.353(7)	Mn2−O17	2.246(8)
Mn1−O1	1.856(6)	Mn2−N2	1.933(8)	Mn1−O1	1.872(6)	Mn2−N2	1.923(8)
Mn1−O13	1.851(6)			Mn1−O24	2.208(7)		
Gd1−O6−Gd2	112.2(3)	Gd2−O13−Mn4	130.1(3)	Dy1−O6−Dy2	112.3(3)	Dy2−O31−Mn4	130.7(3)
Gd2−O13−Mn1	128.8(3)	Mn1−O14−Mn4	91.2(2)	Dy1−O31−Mn1	129.3(3)	Mn1−O31−Mn4	90.7(2)
Gd2−O3−Mn2	123.7(3)	Mn1−O14−Mn4A	105.7(3)	Dy2−O3−Mn2	123.8(3)	Mn1−O28−Mn4A	106.1(3)
Gd2−O12−Mn3	123.8(3)	Mn4−O14−Mn4A	102.5(3)	Dy2−O12−Mn3	124.2(3)	Mn4−O28−Mn4A	101.8(2)

[a]Symmetry code: A, $-x+2, -y+1, -z$; B, $-x+1, -y+1, -z$ for **1**; A, $-x+1, -y+1, -z+1$; B, $-x+1, -y+2, -z+1$ for **2**; A, $-x+1, -y+2, -z+1$; B, $-x, -y, -z+1$ for **3**; $-x+1, -y, -z+2$ for **4**.

using $Tb(NO_3)_3{\cdot}6H_2O$ (0.345 g, 1 mmol) in place of $Eu(NO_3)_3{\cdot}6H_2O$. Yield: 13 mg (28%, based on the ligand). Elem anal. Calcd for $C_{86}H_{126}Cl_8Tb_4Mn_8N_8O_{63}$: C, 28.39; H, 3.49; N, 3.08. Found: C, 28.18; H, 3.65; N, 3.19. IR (KBr, cm^{-1}): 3212(s), 2978(m), 2098(w), 1521(w), 1875(vs), 1215(m), 1789(m), 1231(s), 1687(w), 1687(w), 954(m), 898(m), 718(s), 654(w), 423(w), 475(s).

Synthesis of $[Mn^{III}_8Dy^{III}_4(ClshiH)_8(OAc)_6(\mu_3\text{-}OCH_3)_2(\mu_3\text{-}O)_2(CH_3OH)_{12}(H_2O)_2]{\cdot}4CH_3OH{\cdot}4H_2O$ (4). This compound was obtained as brown block crystals according to the procedure for **1**, using $Dy(NO_3)_3{\cdot}6H_2O$ (0.349 g, 1 mmol) in place of $Eu(NO_3)_3{\cdot}6H_2O$. Yield: 17 mg (32%, based on the ligand). Elem anal. Calcd for $C_{86}H_{124}Cl_8Dy_4Mn_8N_8O_{62}$: C, 28.42; H, 3.43; N, 3.08. Found: C, 28.19; H, 3.63; N, 3.26. IR (KBr, cm^{-1}): 3354(vs), 2785(w), 2135(w), 1786(s), 1868(s), 1535(s), 1789(s), 1453(s), 1657(w), 1546(s), 925(m), 868(m), 786(m), 684(m), 668(m), 438(m).

X-ray Crystallography. Single-crystal X-ray diffraction data for compounds **1**−**4** were collected on a Bruker Smart CCD area-detector diffractometer with Mo Kα radiation (λ = 0.71073 Å) by ω-scan mode operating at room temperature. The program *SAINT* was used for integration of the diffraction profiles, and semiempirical absorption corrections were applied using *SADABS*.[25,26] All of the structures were solved by direct methods using the *SHELXS* program of the *SHELXTL* package and refined by full-matrix least-squares methods with *SHELXL*.[27] Metal ions were located from the *E* maps, and the other non-H atoms were located in successive difference Fourier syntheses and refined with anisotropic thermal parameters on F^2. Generally, C-bound H atoms were determined theoretically and refined with isotropic thermal parameters riding on their parents. H atoms of water and MeOH were first located by difference Fourier *E* maps and then treated isotropically as riding. Further details for crystallography and selected bond parameters are listed in Tables 1 and 2, respectively.

Physical Measurements. Elemental analyses for carbon, hydrogen, and nitrogen were carried out with a Perkin-Elmer 240C elemental analyzer. IR spectra were recorded on a Bruker VECTOR22 FT-IR spectrometer using a KBr pellet technique. Magnetic measurements on crystalline samples were carried out at an applied field of 2 kOe on a Quantum Design MPMS-XL7 superconducting quantum interference device (SQUID) magnetometer working in the temperature range of 300−1.8 K. The molar magnetic susceptibilities were corrected for diamagnetism estimated from Pascal's tables and for the sample holder by previous calibration.

RESULTS AND DISCUSSION

Syntheses. Among the various strategies used in the synthesis of Mn 4f compounds, those using small-nuclearity species with $[Mn_3O]^{6+/7+}$ or $[Mn_4O_2]^{8+}$ cores proved to be fruitful to construct high (≥4)-nuclearity Mn−Ln compounds.[9,13,16−18] In previous documents, a series of Ln_6Mn_6- or Mn-12-MC-4 compounds of salicylhydroxamic acid (shi) were synthesized in MeOH.[28] Also with the same ligand, Pecoraro and co-workers obtained Mn_4Ln_2 compounds with similar 14-MC-5 structure incorporating rare-earth metals into Mn-MC systems. The reactions were carried out in DMF through simple manganese and lanthanide salts.[10d] In this work, however, we obtained the titled compounds by the reaction of

dx.doi.org/10.1021/ic3025952 | Inorg. Chem. 2013, 52, 10747−10755

$Mn(OAc)_2$, $ClshiH_3$, and lanthanide nitrate salts in a 4:4:1 molar ratio in MeOH at room temperature. Apparently, the solvents play an important role in the formation of such compounds.

Additionally, two other important factors may lead to the resulting product. First, a substituted shi ($ClshiH_3$) was employed in our reaction, in which the electronegativity of the Cl atom may influence the electron properties of the ligand and further the assembly of the structure. Second, tetrabutylammonium hydroxide was added in the reaction mixture to adjust the pH value of the solution. The organic base may facilitate deprotonation of the ligand and air oxidation of the manganese(II) starting material.[29]

Description of the Crystal Structures. Single-crystal X-ray structure analysis reveals that all isomorphous compounds crystallize in the space group $P\bar{1}$, presenting two offset stacked symmetry-related 14-MC-5 units. $[Mn_4Dy_2]_2$ (**4**) is described representatively. As shown in Figure 1, each 14-MC-5 unit possesses four Mn^{III} ions, two Dy^{III} ions, four deprotonated 5-$Clshi^{3-}$ ligands, one μ_3-O ion, one μ_3-CH_3OH molecule, and two coordinated carboxylate groups as well as four coordinated water molecules. Phenolate O, carbonyl O, hydroximate O, and imine N atoms of the 5-$Clshi^{3-}$ ligand are all involved in the coordination. In the equatorial plane, four 5-$Clshi^{3-}$ ligands adopt μ_4:η^2:η^1:η^2:η^1 and μ_3:η^1:η^1:η^2:η^1 fashion types to connect four Mn^{III} ions and one Dy^{III} ion to form a new 14-MC-5 cyclic unit with connectivity of [Mn−N−O−Mn−N−O−Ln−O−N−Mn−O−N−Mn−O−]. Mn1, Mn2, Dy1, Mn3, and Mn4 are bridged through M−N−O connectivity in order, while Mn1 and Mn4 are connected by one μ^3-O^{2-} ion, one μ^3-CH_3O^- ion, and one syn−syn carboxylate group of acetate. The Mn−N−O−Mn torsion angles are 179.4(4)° and 176.6(4)° for Mn1−N1−O3−Mn2 and Mn3−O12−N4−Mn4 and the Mn−N−O−Dy torsion angles are −168.7(4)° and +173.4(4)° for Mn2−N2−O6−Dy2 and Mn3−N3−O9−Dy2, respectively.

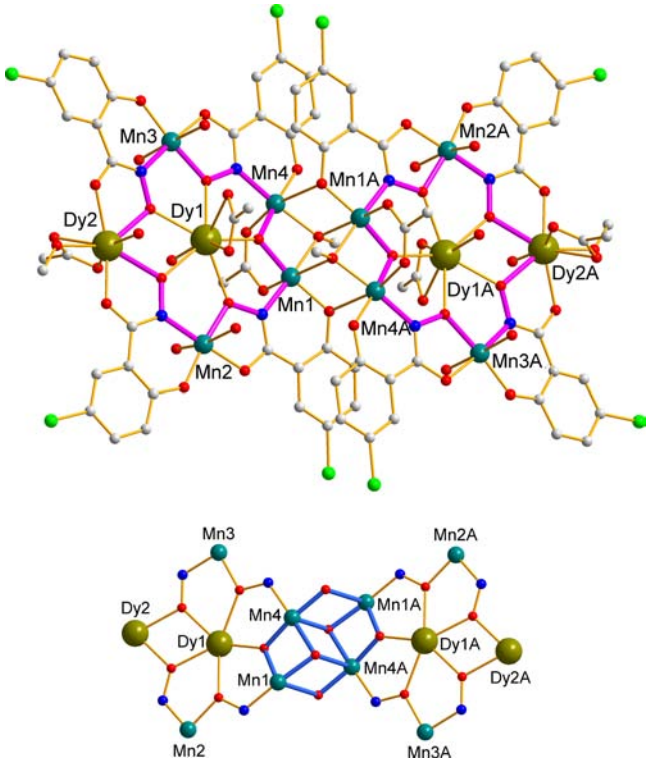

Figure 1. Overall molecular structure and two offset stacked 14-MC-5 cores of **4**, respectively. H atoms have been omitted for clarity. Symmetry code: A, $-x + 1$, $-y$, $-z + 2$.

The oxidation states of Mn ions were deduced from the meric parameters and charge-balance consideration, which was further confirmed by bond valence sum (BVS) calculations (see the Supporting Information, Table S2). All Mn^{III} ions exhibit distorted six-coordinate octahedral geometry, and the JT and apical axes are approximately perpendicular to the MC plane. Two kinds of coordination environments of Mn ions are observed. For Mn1 and Mn4, the equatorial plane is composed of a six-membered iminophenolate ring from one 5-$Clshi^{3-}$ ligand, one μ_3-O^{2-} ion, and one μ_3-CH_3O^- ion. The apical positions are occupied by two O atoms from the carboxylate group and another μ_3-CH_3O^- ion. For Mn2 and Mn3, however, the equatorial plane consists of one six-membered iminophenolate ring and one five-numbered hydroximate ring from different 5-$Clshi^{3-}$ ligands. The axial positions are occupied by MeOH molecules.

The encapsulated Dy1 is surrounded by eight O atoms, four of which in the equatorial plane are from hydroximate of discrete 5-$Clshi^{3-}$ ligands that bridges Mn2, Mn3, and Dy2, while the fifth is from μ_3-O that bridges Mn1 and Mn4. The axial positions are occupied by one acetate group and one aqua molecule. Another lanthanide ion Dy2 on the plane of the molecule is eight-coordinate and bound to two five-membered hydroximate rings, one acetate group, and two MeOH molecules.

Similar monomeric 14-MC-5 compounds were reported very recently by Pecoraro et al. that represent the first M−N−O MC to incorporate both μ-O and μ-OH in the ring and the first MC with the inclusion of one metal that differs from the other ring metals.[10d] Interestingly, in our case, these two 14-MC-5 units are joined together by two μ_3-CH_3O^- groups and two η^2-O of different 5-$Clshi^{3-}$ ligands, forming a unique dimeric structure with two 14-MC-5 in offset stacked mode in which a double Mn_4O_6 cuboidal arrangement is formed. The Mn−O bond distances are in the range of 1.965−2.386 Å, consistent with similar bonds in manganese compounds (1.8−2.3 Å).[29,30] Such a specific bridging mode may provide an opportunity to obtain interesting magnetic properties different from those of structures containing ordinary MCs.

Upon careful inspection of the structure, the dimeric molecules in the compounds could further assemble into a one-dimensional network via intramolecular $\pi\cdots\pi$ stacking interaction (see the Supporting Information, Figure S1). Within each molecule, neighboring 14-MC-5 planes are connected via face-to-face $\pi\cdots\pi$ stacking interactions.

Magnetic Properties. *dc Magnetic Properties.* dc SQUID magnetometry for compounds **1**−**4** was conducted at an applied field of 2000 Oe and in the temperature range of 1.8−300 K. The $\chi_M T$ versus T plots are shown in Figure 2. χ_M is the molar magnetic susceptibility per $[Mn^{III}_4Ln^{III}_2]_2$ dimeric unit. The values of $\chi_M T$ at room temperature were all slightly lower than the expected value with the presence of eight Mn^{III} and four Ln^{III} uncoupled ions, as listed in Table 3. In most of Mn^{III}-based compounds, the room-temperature effective magnetic moment is lower than the theoretical value, assuming $g = 2$. As a matter of fact, the Landé factor of Mn^{III} is lower than 2.0. On the other hand, antiferromagnetic coupling between metal ions also leads to a smaller value than the theoretical magnetic moment. All compounds in this manuscript exhibit antiferromangetic coupling between two $[Mn_4Ln_2]$ units, leading to

dx.doi.org/10.1021/ic3025952 | Inorg. Chem. 2013, 52, 10747−10755

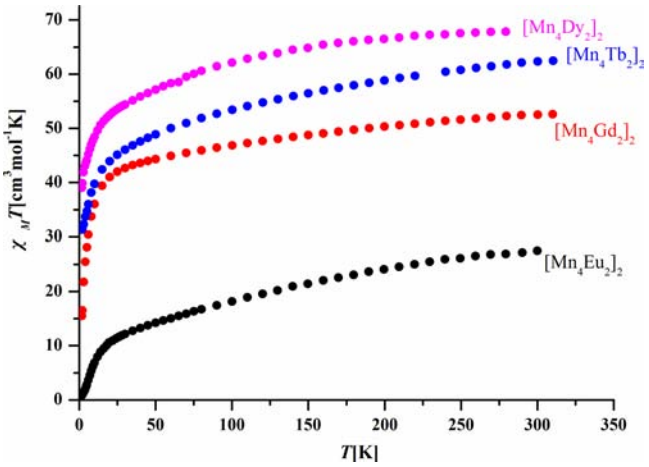

Figure 2. $\chi_M T$ versus T plots for **1**–**4** at 2000 Oe.

Table 3. Expected and Measured χT Values (cm^3 K mol^{-1}) for Dimeric $[Mn_4Ln_2]_2$ and Monomeric $[Mn_4Ln_2]$ at 300 K

		$[Mn_4Ln_2]_2$ in this work		$[Mn_4Ln_2]$ in ref 10d	
trivalent lanthanide ion	theoretical value for a single ion	expected value	measured value	expected value	measured value
Eu (**1**)	1.50	30.00	27.74		
Gd (**2**)	7.88	55.52	54.95	27.76	25
Tb (**3**)	11.82	71.28	62.83	35.64	27
Dy (**4**)	14.17	80.68	71.72	40.34	36

a slight decrease of the magnetic moment. So, these two effects make the $\chi_M T$ values lower in all compounds. Similar phenomena were also observed in the monomeric structures. Upon lowering of the temperature, these values decreased steadily. From 50 K, the values decreased rapidly and reached 0.86 [for $[Mn_4Eu_2]_2$ (**1**)], 16.19 [for $[Mn_4Gd_2]_2$ (**2**)], 31.48 [for $[Mn_4Tb_2]_2$ (**3**)], and 41.23 cm^3 K mol^{-1} (for **4**) at 1.8 K, respectively. Such behavior indicates that antiferromagnetic interaction between the metal centers dominates the magnetic properties of **1**–**4**.

Similar to other Mn-4f compounds, the magnetic behavior of this family of compounds also combines the Mn^{III}–Mn^{III}, Mn^{III}–Ln^{III}, and Ln^{III}–Ln^{III} interactions in addition to the intrinsic magnetic properties of the Ln^{III} ions. For compound **1** containing the Eu^{III} ion, we may try investigating the magnetic interaction mode between metal ions, while for other compounds, it is difficult to define.

The Eu^{III} ion has a $^7F_0$ ground state with a $4f^6$ configuration ($^7F_0$, $S = 3$, $L = 3$, $J = 0$). At low temperature, only the nonmagnetic ground level is occupied with the infinitesimal excited states mixing into $^7F_0$.[31] Therefore, the low-temperature magnetic properties of compound **1** are only dominated by the exchange interaction between Mn^{III} ions. This means that the Eu^{III} ions can be considered as the diamagnetic centers at low temperatures. On the basis of the low-temperature $\chi_M T$ values and the extrapolation at 0 K, which is approaching zero, the ground-state spin of **1** can be determined to be $S = 0$. Thus, we can draw a conclusion that the antiferromagnetic behavior of **1** is attributed to the combination of Mn^{III}–Mn^{III} interaction within and between two $[Mn_4]$ units. For other compounds that also possess antiferromagnetic $[Mn_4]_2$ units, the nonzero ground-state spins may result from the contribution of uncanceled spins between the $[Mn_4]_2$ units and Ln^{III} ions as well as the single-ion magnetoanisotropy of Ln^{III} ions. Because of the presence of a large orbital contribution from the 4f ions and the complexity of the magnetic coupling interactions within these compounds, fitting the data to obtain the coupling constants is not feasible.

As shown in Figure 3, the dc magnetization data of the compounds were carried out in the ranges of magnetic field from 1 to 7 T and temperature from 10 to 1.8 K, respectively. These compounds exhibit similar behavior with an increase at low field and then a linear increase without clear saturation at 7 T with values of 10.78 μ_B for **1**, 39.64 μ_B for **2**, 30.00 μ_B for **3**, and 29.36 μ_B for **4**. As for the reduced magnetization ($M/N\mu_B - H/T$) curves, the nonsuperimposition properties of all of the compounds suggest the presence of magnetic anisotropy and the lack of a well-defined ground state.

Alternating-Current (ac) Magnetic Properties. To probe the dynamics of magnetization relaxation, ac susceptibility measurements were performed in a zero applied dc field with a 5.0 Oe ac field oscillating at frequencies in the range of 1–1500 Hz and in the temperature range of 1.8–10.0 K. Except for **4**, other compounds do not exhibit any out-of-phase ac signals (see the Supporting Information, Figure S3).

The in-phase $\chi'_M T$ signal of **4** showed a frequency-dependent decrease at $T < 4$ K, indicating the presence of slow magnetization relaxation and thus probably SMM behavior. The out-of-phase χ''_M signals showed weak frequency dependence (Figure 4a,b). The maxima of these signals, however, were not observed above 1.8 K, the lowest limit of the instrument. Consequently, the effective energy barrier (U_{eff}) and the magnetization relaxation time (τ) could not be determined. Owing to the extremely low blocking temperature, the hysteresis experiments could not also be performed to definitively characterize the compound as SMM.

It should be noted that when the dc field increased to 2 kOe, the frequency-dependent properties increased and significant maxima of the peaks were observed (Figure 4c,d). The Cole–Cole plot of the in-phase (χ'_M) versus out-of-phase (χ''_M) signal of the ac magnetic susceptibility exhibits two interesting relaxation phases at a dc field of 2 kOe (Figure 5). The relaxation time for each process can be extracted by fitting the data to two relaxation processes using the sum of two modified Debye functions:[32]

$$\chi_{ac}(\omega) = \chi_{S,tot} + \frac{\Delta\chi_1}{1 + (i\omega\tau_1)^{1-\alpha_1}} + \frac{\Delta\chi_2}{1 + (i\omega\tau_2)^{1-\alpha_2}},$$

$$\omega = 2\pi\nu$$

where $\chi_{S,tot} = \chi_{S1} + \chi_{S2}$ represents the sum of the adiabatic susceptibilities of the two relaxing species; $\Delta\chi_i$ is the difference between the adiabatic susceptibility (χ_{Si}) and the isothermal susceptibility (χ_{Ti}) of each magnetic phase. The experimental $\chi_{ac}(\omega)$ curves between 1.8 and 3.0 K can be nicely simulated by applying the equation and depicted as $\chi'(\omega)$ and $\chi''(\omega)$. The simulations of dynamical susceptibility ranging from 1.8 to 3.0 K are shown in Figures 5 and S2 in the Supporting Information, respectively. The fitting parameters obtained are summarized in Table S1 in the Supporting Information.

From the Cole–Cole plot, a conclusion can be drawn that compound **4** displays closely spaced relaxation pathways under an applied dc field. A two-step relaxation process illustrates that two relaxation phases could be separated into two parts: a high-frequency domain at frequencies from 10 to 1500 Hz and a low-frequency domain at frequencies from 1 to 6.8 Hz. Thus, the parameters α and τ are obtained by Debye simulation

dx.doi.org/10.1021/ic3025952 | Inorg. Chem. 2013, 52, 10747–10755

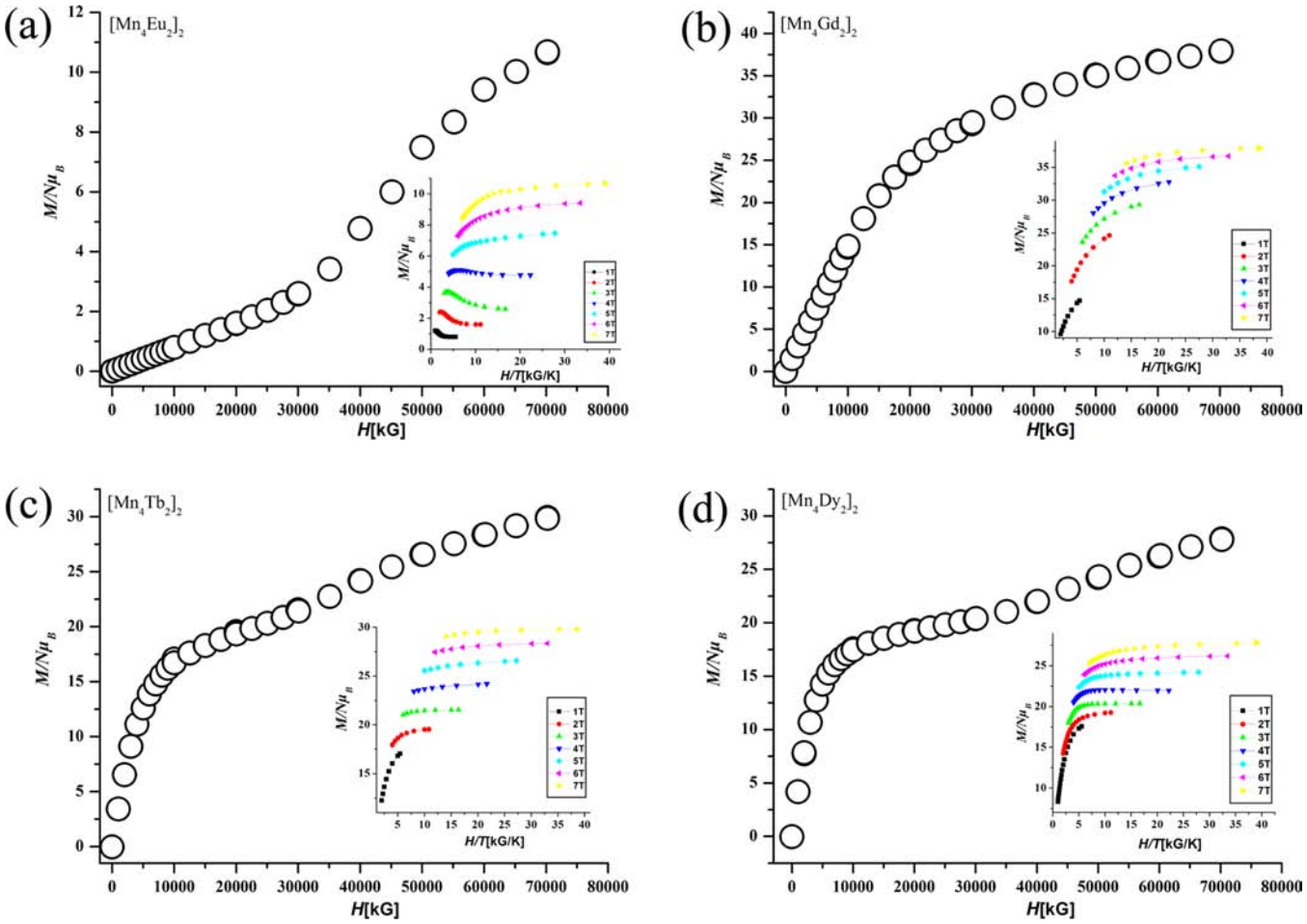

Figure 3. Plot of the field-dependent magnetization and reduced magnetization (insets) of **1**−**4** at the indicated applied fields and temperatures. The solid lines are guides for the eyes.

quantifying the width of the τ distribution and the relaxation time, respectively. The parameter α_1 increases but α_2 decreases with heating, and the relaxation time τ_1 is much larger than τ_2. Both of the differences of parameters α and τ indicate two different relaxation mechanisms in the spin reversal of the compound. On the basis of the above analysis, the right incomplete part corresponding to a low-frequency domain could be assigned to slower relaxation (SR) dynamics with parameters α_1 and τ_1 and the left semicircles corresponding to a high-frequency one are the faster relaxation (FR) dynamics with parameters α_2 and τ_2. Long et al. have recently reported the observation of a secondary slow relaxation process for the field-induced SMM.[33] They calculated this by fitting the data of each individual relaxation domain using a generalized Debye model. Similar results were observed in which the α parameters changed with opposite tendencies while the temperature changed and the relaxation times τ were different between the FR and SR domains. Because of the complexity of the relaxation mechanism of lanthanide ions and the differences between single lanthanide ion magnetic behavior and that of the transition-metal-cluster SMMs, further characterization of this system will require measurements at lower frequencies and temperatures to investigate the multiple relaxation pathways in detail.[34]

According to Long's work, magnetic measurements indicated that, as the dc field is increased, the asymmetry in the Cole−Cole plot disappears and a smooth semicircular arc is observed. The increasing dc field could eliminate one of the relaxation processes to remove the asymmetry of the overall Cole−Cole curve. Similar field-induced SMM or SIM behavior was investigated in the presence of nonzero dc fields. The origin of the field-induced relaxation behavior could be attributed to suppressed fast quantum tunneling of magnetization by applied dc fields. Similar phenomena have also been observed in recent compounds.[35]

In a previous manuscript of Pecoraro, the authors reported the isostructural Y, Gd, Tb, Dy, and Ho monomeric 14-MC-5. In five structures, the latter three examples displayed slow magnetic relaxation, while the former two examples did not and the Dy compound exhibited the highest blocking temperature. In our dimeric 14-MC-5, however, only the Dy example showed magnetic dependence upon the frequencies at nonzero field. That is, optimal behavior was observed in the Dy^{III} compound, and similar phenomena have been found in other series of compounds.[36] This may be explained by the intrinsic properties of trivalent Ln^{III} ions. The Kramers ion Dy^{III} could always maintain the doubly degenerate ground state under the magnetic field in most of coordination environment. The non-Kramers ion, Tb^{III}, however, needs a strictly axial crystal-field symmetry. Additionally, the Eu^{III} ion has a $J = 0$ ground state, while the Gd^{III} ion is isotropic.

Compared to other similar monomeric Mn_4Dy_2-14-MC-5 compounds exhibiting strong frequency dependence at all frequencies in a zero dc field, the SMM property of the $[Mn_8Dy_2]_2$ compound in this work is apparently weakened. Two major reasons should be taken into account to interpret

dx.doi.org/10.1021/ic3025952 | Inorg. Chem. 2013, 52, 10747−10755

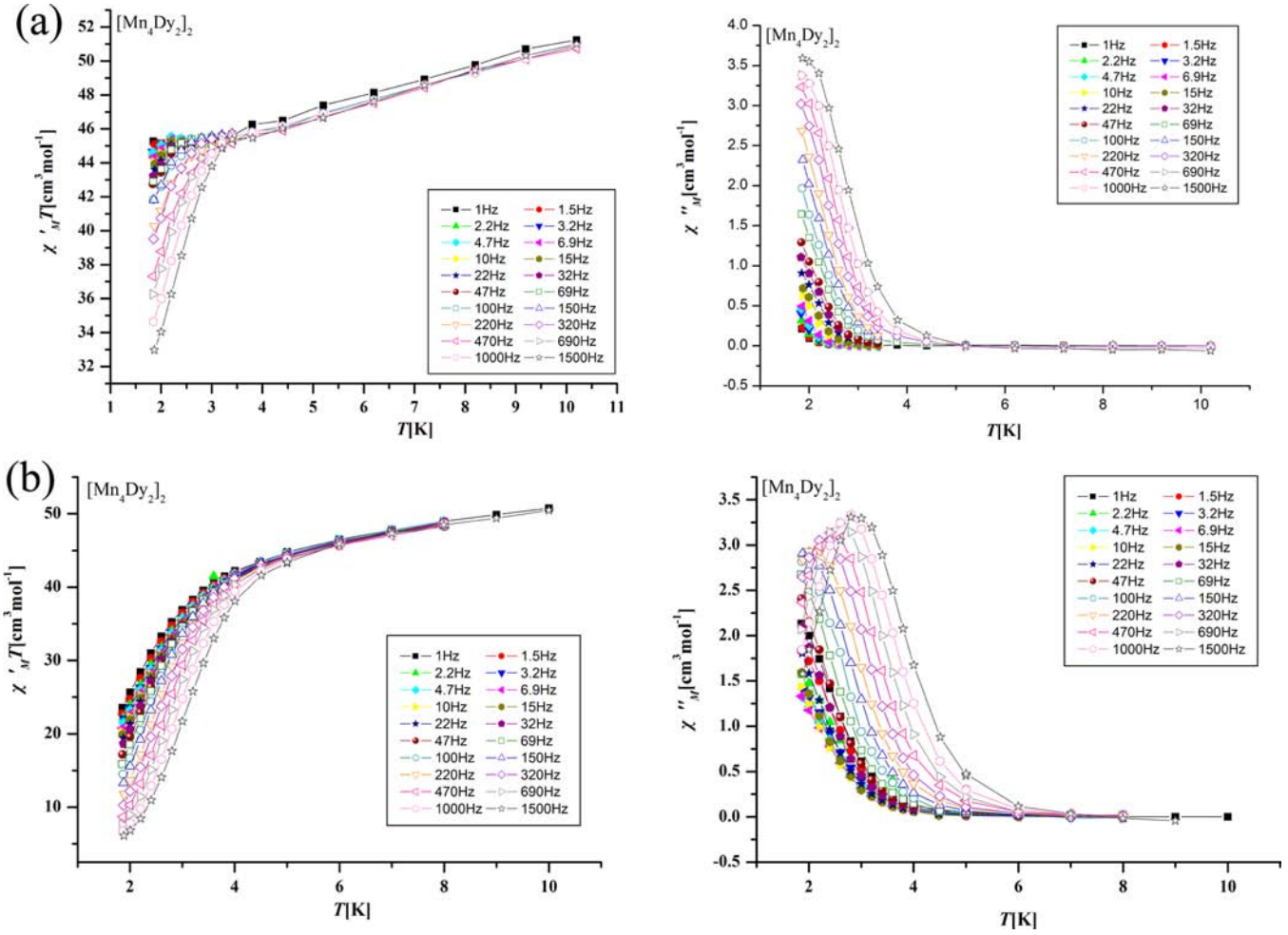

Figure 4. Plots of the in-phase (χ'_M) and out-of-phase (χ''_M) signals for **4** in ac susceptibility studies versus T in a 5.0 Oe field with a zero dc field (a) compared to an applied dc field of 2 kOe (b). The solid lines are guides for the eyes.

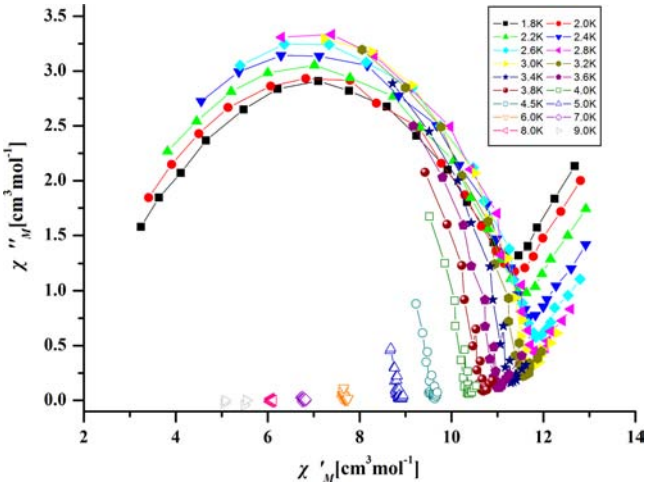

Figure 5. Plots of the in-phase (χ'_M) versus out-of-phase (χ''_M) signals for **4** in ac susceptibility studies in a 5.0 Oe field under an applied dc field of 2000 Oe. The solid lines are guides for the eyes.

the weak magnetic properties of the dimer compared to the monomer. One is the probable antiferromagnetic interactions within the planar MC rings. The second is the antiferromagnetic coupling interactions at the junction of two MC rings, which are related to the Mn^{III}–O(R)–Mn^{III} angles.

Pecoraro and co-workers had reported that the planarity of the MC ring was very important to preclude the likelihood of anisotropy vectors of each single metal ion canceling each other to decrease the integrated anisotropy of the whole molecule. The important geometry parameters of the monomeric 14-MC-5 and dimeric 14-MC-5 compounds in this work are listed in Figure S4 in the Supporting Information. One can see that the metal···metal distances between the metal ions within these structures were similar. A side view of the two MC rings, however, showed different planarity. In the monomeric 14-MC-5 structure, the Dy^{III} ion within the MC ring (Dy1) and the encapsulated (Dy2) Dy^{III} ion are 1.734 and 0.300 Å above the MC plane, respectively. In the dimeric structure of this work, these Dy^{III} ions are 0.113 and 0.402 Å below and above the MC plane, respectively. Additionally, the coordination geometries around the Dy^{III} ions in both structures are different because one acetate bridged both of the Dy^{III} ions in the monomer, which could be related to the differences of the deviation between the Dy^{III} ions and the MC plane.

The skeleton structure of the dimer showed a higher planarity than that of the monomer. The planar MC ring always shows antiferromagnetic coupling between metal ions within the ring, so the ground-state spin is low.[37] In contrast, a nonplanar MC ring provides ferromagnetic coupling between metal ions, and the compound will have a higher ground-state spin. According to $U_{eff} = |D|S^2$, the energy barrier of the dimer

dx.doi.org/10.1021/ic3025952 | Inorg. Chem. 2013, 52, 10747−10755

should be lower than that of the monomer, further leading to frequency-dependent signals of **4** in this work in lower temperature. So, the signals can be observed under the required applied field. Thus, we could conclude that the planarity of the MC ring is the origin of different magnetic properties between the monomer and dimer.

Second, antiferromagnetic coupling could usually quench the SMM properties because of the reduced ground-state spin. In **4**, two 14-MC-5 units were connected by two μ_3-CH_3O^- groups and two η^2-O atoms of different 5-Clshi^{3-} ligands with four Mn ions and six O atoms in a double Mn_4O_6 cubane arrangement. Generally, Mn^{III}–O(R)–Mn^{III} angles smaller than about 102° tend to favor ferromagnetic exchange interactions.[38,39] In this double cubane, the Mn–O–Mn angles are in the range of 101.82–106.11°, indicating antiferromagnetic interaction within the Mn^{III} ions. Considering a similar analysis investigated by Christou and co-workers with respect to offset stacked 9-MC-3, one can see that the Mn^{III}–O(R)–Mn^{III} angles in the junction of two MC rings in these compounds are all smaller than 102°, resulting in ferromagnetic interactions between the MC rings.[40] It is remarkable that π–π intramolecular interaction between the two offset stacked MC rings could explain the different Mn^{III}–O(R)–Mn^{III} angles between the monomer and dimer.

From these experiments, one can see the importance of the choice of Ln^{III} on the SMM properties. Powell, Pecoraro, and other groups have also performed systematic investigations on the family of isomorphous compounds, showing that the slow magnetic relaxation behavior of the compound depends on both the spin and anisotropy components of Ln^{III}.[9−11] They also reported that the Dy^{III} ion may have the right "blend" of spin and anisotropy needed for effective SMMs. In our case, the Dy^{III} analogue showed slow magnetization relaxation, consistent with previous investigations; even the SMM properties were decreased compared with monomeric 14-MC-5.

CONCLUSION

In summary, the use of $ClshiH_3$ in reactions with manganese and lanthanide salts results in the formation of a new family of 3d–4f dodenuclear compounds with the lanthanide ions in the MC ring, each containing two offset stacked 14-MC-5 units with M–N–O–M–N–O–Ln–O–N–M–O–N–M connectivity. The magnetic behavior of the family of compounds was discussed in detail including the Mn^{III}–Mn^{III}, Mn^{III}–Ln^{III}, and Ln^{III}–Ln^{III} interactions. Mn^{III}–Mn^{III} interaction within and between the units in all compounds may be antiferromagnetic. The nonzero ground states of compounds **2**–**4** are the result of uncanceled net spins between the Ln^{III} and Mn^{III} ions. The Dy^{III} analogue with high anisotropy and large spin shows slow magnetization relaxation at a dc field of 2 kOe. The effect of the planarity of the MC, the choice of Ln^{III} ions, and the connectivity of the two MCs are discussed in detail.

ASSOCIATED CONTENT

Supporting Information

Experimental procedures, crystal structure data of **1**–**4**, crystallographic data for **1**–**4** in CIF format, and a table of BVS calculations. This material is available free of charge via the Internet at http://pubs.acs.org. Crystallographic data for structural analysis of the compounds have also been deposited with the Cambridge Crystallographic Data Centre, under CCDC 850415–850418. Copies of this information may be obtained free of charge from The Director, CCDC, 12 Union Road, Cambridge CB2 1EZ, U.K. (http://www.ccdc.cam.ac.uk; fax +44-1223-762911).

AUTHOR INFORMATION

Corresponding Authors

*E-mail: yousong@nju.edu.cn.
*E-mail: jmdou@lcu.edu.cn.

Notes

The authors declare no competing financial interest.

ACKNOWLEDGMENTS

We are thankful to the National Natural Science Foundation of China (Grants 21271097 and 21141003) and Liaocheng University for financial support. We are thankful to the National Natural Science Foundation of China (Grants 21271097 and 21141003) for financial support.

REFERENCES

(1) (a) Pecoraro, V. L. *Inorg. Chim. Acta* **1989**, *155*, 171. (b) Lah, M. S.; Pecoraro, V. L. *J. Am. Chem. Soc.* **1990**, *11*, 59.

(2) (a) Pecoraro, V. L.; Stemmler, A. J.; Gibney, B. R.; Wang, H.; Kampf, J. W.; Barwinski, A. *Prog. Inorg. Chem.* **1997**, *45*, 83. (b) Bodwin, J. J.; Cutland-Van Noord, A. D.; Malkani, G. R.; Pecoraro, V. L. *Coord. Chem. Rev.* **2001**, *216–217*, 489. (c) Mezei, G.; Zaleski, C. M.; Pecoraro, V. L. *Chem. Rev.* **2007**, *107*, 4933.

(3) (a) Zaleski, C. M.; Depperman, E. C.; Kampf, J. W.; Kirk, M. L.; Pecoraro, V. L. *Inorg. Chem.* **2006**, *45*, 10022. (b) Zaleski, C. M.; Kampf, J. W.; Mallah, T.; Kirk, M. L.; Pecoraro, V. L. *Inorg. Chem.* **2007**, *46*, 1954. (c) Xu, H. B.; Wang, B. W.; Pan, F.; Wang, Z. M.; Gao, S. *Angew. Chem., Int. Ed.* **2007**, *47*, 7388.

(4) (a) Sessoli, R.; Gatteschi, D.; Novak, M. A. *Nature* **1993**, *365*, 141. (b) Sessoli, R.; Tsai, H.; Schake, A. R.; Wang, S.; Vincent, J. B.; Folting, K.; Gatteschi, D.; Christou, G.; Hendrickson, D. N. *J. Am. Chem. Soc.* **1993**, *115*, 1804.

(5) (a) Aromil, G.; Brechin, E. K. *Struct. Bonding (Berlin)* **2006**, *122*, 1. (b) Christou, G. *Polyhedron* **2005**, *24*, 2065. (c) Roubeau, O.; Clérac, R. *Eur. J. Inorg. Chem.* **2008**, 4325. (d) Tasiopoulos, A. J.; Perlepes, S. P. *Dalton Trans.* **2008**, 5537. (e) Bagai, R.; Christou, G. *Chem. Soc. Rev.* **2009**, *38*, 1011. (f) Stamatatos, T. C.; Christou, G. *Inorg. Chem.* **2009**, *48*, 3308.

(6) Dendrinou-Samara, C.; Alexiou, M.; Zaleski, C. M.; Kampf, J. W.; Kirk, M. L.; Kessissoglou, D. P.; Pecoraro, V. L. *Angew. Chem., Int. Ed.* **2003**, *42*, 3763.

(7) Zaleski, C. M.; Depperman, E. C.; Dendrinou-Samara, C.; Alexiou, M.; Kampf, J. W.; Kessissoglou, D. P.; Kirk, M. L.; Pecoraro, V. L. *J. Am. Chem. Soc.* **2005**, *127*, 12862.

(8) (a) Aldamen, M. A.; Clemente-Juan, J. M.; Coronado, E.; Martí-Gastaldo, C.; Gaita-Arino, A. *J. Am. Chem. Soc.* **2008**, *130*, 8874. (b) Ishikawa, N.; Sugita, M.; Ishikawa, T.; Koshihara, S.-y.; Kaizu, Y. *J. Am. Chem. Soc.* **2003**, *125*, 8694.

(9) (a) Mereacre, V.; Lan, Y.; Clerac, R.; Ako, A. M.; Hewitt, I. J.; Wernsdorfer, W.; Buth, G.; Anson, C. E.; Powell, A. K. *Inorg. Chem.* **2010**, *49*, 5293. (b) Ako, A. M.; Lan, Y. H.; Clérac, R.; Wernsdorfer, W.; Hewitt, I. J.; Anson, C. E.; Mereacre, V.; Anson, C. E.; Powell, A. K. *Polyhedron* **2009**, *28*, 1698. (c) Mishra, A.; Wernsdorfer, W.; Parson, S.; Christou, G.; Brechin, E. K. *Chem. Commun.* **2005**, 2086. (d) Akhtar, M. N.; Zheng, Y. Z.; Lan, Y. H.; Mereacre, V.; Anson, C. E.; Powell, A. K. *Inorg. Chem.* **2009**, *48*, 3502. (e) Lampropoulos, C.; Stamatatos, T. C.; Abboud, K. A.; Christou, G. *Inorg. Chem.* **2009**, *48*, 429. (f) Prasad, T. K.; Rajasekharan, M. V.; Costes, J. P. *Angew. Chem., Int. Ed.* **2007**, *46*, 2851. (g) Guedes, G. P.; Soriano, S.; Mercante, L. A.; Speziali, N. L.; Novak, M. A.; Andruh, M.; Vaz, M. G. F. *Inorg. Chem.* **2013**, *52*, 8309. (h) Chandrasekhar, V.; Bag, P.; Speldrich, M.; Leusen, J.; Kögerler, P. *Inorg. Chem.* **2013**, *52*, 5035. (i) Feuersenger, J.; Prodius, D.; Mereacre, V.; Clérac, R.; Anson, C. E.; Powell, A. K. *Inorg. Chem. Commun.* **2011**, *14*, 1851. (j) Chilton, N. F.; Langley, S. K.; Moubaraki, B.; Murray, K. S. *Chem. Commun.* **2010**, *46*, 7787.

(10) (a) Karotsis, G.; Kennedy, S.; Teat, S. J.; Beavers, C. M.; Fowler, D. A.; Morales, J. J.; Evangelisti, M.; Dalgarno, S. J.; Brechin, E. K. *J. Am. Chem. Soc.* **2010**, *132*, 12983. (b) Mereacre, V.; Akhtar, M. N.;

Lan, Y. H.; Ako, A. M.; Clérac, R.; Anson, C. E.; Powell, A. K. *Dalton Trans.* **2010**, *39*, 4918. (c) Shiga, T.; Hoshino, N.; Nakano, M.; Nojiri, H.; Oshio, H. *Inorg. Chim. Acta* **2008**, *361*, 4113. (d) Boron, T. T., III; Kampf, J. W.; Pecoraro, V. L. *Inorg. Chem.* **2010**, *49*, 9104. (e) Liu, C. M.; Zhang, D. Q.; Zhu, D. B. *Dalton Trans.* **2010**, *39*, 11325. (f) Li, M.; Ako, A. M.; Lan, Y.; Wernsdorfer, W.; Buth, G.; Anson, C. E.; Powell, A. K.; Wang, Z.; Gao, S. *Dalton Trans.* **2010**, *39*, 3375. (g) Majeed, Z.; Mondal, K. C.; Kostakis, G. E.; Lan, Y.; Anson, C. E.; Powell, A. K. *Dalton Trans.* **2010**, *39*, 4740. (h) Karotsis, G.; Evangelisti, M.; Dalgarno, S. J.; Brechin, E. K. *Angew. Chem., Int. Ed.* **2009**, *48*, 9928.

(11) (a) Mereacre, V.; Ako, M. A.; Clérac, R.; Wernsdorfer, W.; Hewitt, I.; Anson, C. E.; Powell, A. K. *Chem.—Eur. J.* **2008**, *14*, 3577. (b) Shiga, T.; Onuki, T.; Matsumoto, T.; Nojiri, H.; Newton, G. N.; Hoshino, N.; Oshio, H. *Chem. Commun.* **2009**, 3568. (c) Ako, A. M.; Mereacre, V.; Clérac, R.; Hewitt, I. J.; Lan, Y.; Buth, G.; Anson, C. E.; Powell, A. K. *Inorg. Chem.* **2009**, *48*, 6713.

(12) (a) Rigaux, G.; Inglis, R.; Morrison, S.; Prescimone, M.; Brechin, E. K. *Dalton Trans.* **2011**, *40*, 4797. (b) Holyńska, M.; Premužić, D.; Jeon, I.; Wernsdorfer, W.; Clérac, R.; Dehnen, S. *Chem.—Eur. J.* **2011**, *17*, 9605. (c) Zaleski, C. M.; Kampf, J. W.; Mallah, T.; Kirk, M. L.; Pecoraro, V. L. *Inorg. Chem.* **2007**, *46*, 1954. (d) Wang, M.; Yuan, D. Q.; Ma, C. B.; Yuan, M. J.; Hu, M. Q.; Li, N.; Chen, H.; Chen, C. N.; Liu, Q. T. *Dalton Trans.* **2010**, *39*, 7276.

(13) Zaleski, C. M.; Depperman, E. C.; Kampf, J. W.; Kirk, M. L.; Pecoraro, V. L. *Angew. Chem., Int. Ed.* **2004**, *43*, 3912.

(14) Mishra, A.; Tasiopoulos, A. J.; Wernsdorfer, W.; Moushi, E. E.; Moulton, B.; Zaworotko, M. J.; Abboud, K. A.; Christou, G. *Inorg. Chem.* **2008**, *47*, 4832.

(15) Langlry, S. K.; Moubaraki, B.; Murray, K. S. *Dalton Trans.* **2010**, *39*, 5066.

(16) Mereacre, V.; Prodius, D.; Ako, A. M.; Kaur, N.; Lipkowski, J.; Simmons, C.; Dalal, N.; Geru, I.; Anson, C. E.; Powell, A. K.; Turta, C. *Polyhedron* **2008**, *27*, 2459.

(17) (a) Mishra, A.; Wernsdorfer, W.; Abboud, K.; Christou, G. *J. Am. Chem. Soc.* **2004**, *126*, 15648. (b) Mereacre, V.; Ayuk, A. M.; Clérac, R.; Wernsdorfer, W.; Filoti, G.; Bartolomé, J.; Anson, C. E.; Powell, A. K. *J. Am. Chem. Soc.* **2007**, *129*, 9248.

(18) (a) Stamatatos, T. C.; Teat, S. J.; Wernsdorfer, W.; Christou, G. *Angew. Chem., Int. Ed.* **2009**, *48*, 521. (b) Liu, J. L.; Guo, F. S.; Meng, Z. S.; Zheng, Y. Z.; Leng, J. D.; Tong, M. L.; Ungur, L.; Chibotaru, L. F.; Herouxc, K. J.; Hendrickson, D. N. *Chem. Sci.* **2011**, *2*, 1268.

(19) Ako, A. M.; Mereacre, V.; Clérac, R.; Wernsdorfer, W.; Hewitt, I.; Anson, C. E.; Powell, A. K. *Chem. Commun.* **2009**, 544.

(20) Papatriantafyllopoulou, C.; Wernsdorfer, W.; Abboud, K. A.; Christou, G. *Inorg. Chem.* **2011**, *50*, 421.

(21) Zaleski, C. M.; Tricard, S.; Depperman, E. C.; Wernsdorfer, W.; Mallah, T.; Kirk, M. L.; Pecoraro, V. L. *Inorg. Chem.* **2011**, *50*, 11348.

(22) (a) Dou, J. M.; Liu, M. L.; Li, D. C.; Wang, D. Q. *Eur. J. Inorg. Chem.* **2006**, 4866. (b) Chen, Y. T.; Dou, J. M.; Li, D. C.; Wang, S. N.; Wang, D. Q. *Inorg. Chem. Commun.* **2010**, *13*, 167. (c) Zhao, X. J.; Li, D. C.; Zhang, Q. F.; Wang, D. Q.; Dou, J. M. *Inorg. Chem. Commun.* **2010**, *13*, 346. (d) Shi, X. F.; Li, D. C.; Wang, S. N.; Zeng, S. Y.; Wang, D. Q.; Dou, J. M. *J. Solid State Chem.* **2010**, *183*, 2144.

(23) Wang, S. N.; Kong, L. Q.; Yang, H.; He, Z. T.; Jiang, Z.; Li, D. C.; Zeng, S. Y.; Niu, M. J.; Song, Y.; Dou, J. M. *Inorg. Chem.* **2011**, *50*, 2705.

(24) Chen, J. Q. *Nonferrous Met.* **1987**, *3*, 26.

(25) *SAINT v5.0-6.01*; Bruker Analytical X-ray Systems Inc.: Madison, WI, 1998.

(26) Sheldrick, G. M. *SADABS*; University of Göttingen: Göttingen, Germany.

(27) *SHELXTL v5.1*, Bruker Analytical X-ray Systems Inc.: Madison, WI, 1999.

(28) Dendrinou-Samara, C.; Papadopoulos, A. N.; Malamatari, D. A.; Tarushi, A.; Raptopoulou, C. P.; Terzis, A.; Samaras, E.; Kessissoglou, D. P. *J. Inorg. Biochem.* **2005**, *99*, 864.

(29) Chen, H.; Ma, C. B.; Yan, D. Q.; Hu, M. Q.; Wen, H. M.; Liu, Q. T.; Chen, C. N. *Inorg. Chem.* **2011**, *50*, 10342.

(30) (a) Sānudo, E. C.; Grillo, V. A.; Knapp, M. J.; Bollinger, J. C.; Huffman, J. C.; Hendrickson, D. N.; Christou, G. *Inorg. Chem.* **2002**, *41*, 2441. (b) Ghachtouli, S. E.; Guillot, R.; Aukauloo, A.; Dorlet, P.; Anxolabehére-Mallart, E.; Costentin, C. *Inorg. Chem.* **2012**, *51*, 3603. (c) Naiya, S.; Biswas, S.; Drew, M. G. B.; Gómez-García, C. J.; Ghosh, A. *Inorg. Chem.* **2012**, *51*, 5332. (d) Stamatatos, T. C.; Luisi, B. S.; Moulton, B.; Christou, G. *Inorg. Chem.* **2008**, *47*, 1134.

(31) Wan, Y. H.; Zhang, L. P.; Jin, L. P.; Gao, S.; Lu, S. Z. *Inorg. Chem.* **2003**, *42*, 4985.

(32) Grahl, M.; Kotzler, J.; Sessler, I. *J. Magn. Magn. Mater.* **1990**, *90−1*, 187.

(33) Rinehart, J. D.; Meihaus, K. R.; Long, J. R. *J. Am. Chem. Soc.* **2010**, *132*, 7572.

(34) Ishikawa, N.; Sugita, M.; Ishikawa, T.; Koshihara, S.; Kaizu, Y. *J. Phys. Chem. B* **2004**, *108*, 11265.

(35) (a) Li, D.; Parkin, S.; Wang, G.; Yee, G. T.; Clérac, R.; Wernsdorfer, W.; Holmes, S. M. *J. Am. Chem. Soc.* **2006**, *128*, 4214. (b) Bhunia, A.; Gamer, M. T.; Ungur, L.; Chibotaru, L. F.; Powell, A. K.; Lan, Y.; Roesky, P. W.; Menges, F.; Riehn, C.; Niedner-Schatteburg, G. *Inorg. Chem.* **2012**, *51*, 9589. (c) Liu, J. L.; Yuan, K.; Leng, J. D.; Ungur, L.; Wernsdorfer, W.; Guo, F. S.; Chibotaru, L. F.; Tong, M. L. *Inorg. Chem.* **2012**, *51*, 8538. (d) Vallejo, J.; Castro, I.; Ruiz-García, R.; Cano, J.; Julve, M.; Lloret, F.; Munno, G. D.; Wernsdorfer, W.; Pardo, E. *J. Am. Chem. Soc.* **2012**, *134*, 15704. (e) Liu, S. J.; Zhao, J. P.; Song, W. C.; Han, S. D.; Liu, Z. Y.; Bu, X. H. *Inorg. Chem.* **2013**, *52*, 2103.

(36) Rinehart, J. D.; Long, J. R. *Chem. Sci.* **2011**, *2*, 2078.

(37) (a) Milios, C. J.; Piligkos, S.; Brechin, E. K. *Dalton Trans.* **2008**, 1809. (b) Milios, C. J.; Vinslava, A.; Wood, P. A.; Parsons, S.; Wernsdorfer, W.; Christou, G.; Perlepes, S. P.; Brechin, E. K. *J. Am. Chem. Soc.* **2007**, *129*, 8. (c) Cano, J.; Cauchy, T.; Ruiz, E.; Milios, C. J.; Stoumpos, C. C.; Stamatatos, T. C.; Perlepes, S. P.; Christou, G.; Brechin, E. K. *Dalton Trans.* **2008**, 234. (d) Milios, C. J.; Vinslava, A.; Wernsdorfer, W.; Moggach, S.; Parsons, S.; Perlepes, S. P.; Christou, G.; Brechin, E. K. *J. Am. Chem. Soc.* **2007**, *129*, 2754. (e) Yang, C. I.; Cheng, K. H.; Hung, S. P.; Nakano, M.; Tsai, H. L. *Polyhedron* **2011**, *30*, 3272. (f) Yang, C. I.; Wernsdorfer, W.; Cheng, K. H.; Nakano, M.; Lee, G. H.; Tsai, H. L. *Inorg. Chem.* **2008**, *47*, 10184.

(38) Miyasaka, H.; Clérac, R.; Mizushima, K.; Sugiura, K.; Yamashita, M.; Wernsdorfer, W.; Coulon, C. *Inorg. Chem.* **2003**, *42*, 8203.

(39) Miyasaka, H.; Clerac, R.; Ishii, T.; Chang, H. C.; Kitagawa, S.; Yamashita, M. *J. Chem. Soc., Dalton Trans.* **2002**, 1528.

(40) (a) Yang, C. I.; Cheng, K. H.; Nakano, M.; Lee, G. H.; Tsai, H. L. *Polyhedron* **2009**, *28*, 1842. (b) Yang, C. I.; Tsai, Y. J.; Hung, S. P.; Tsai, H. L.; Nakano, M. *Chem. Commun.* **2010**, *46*, 5716. (c) Yang, C. I.; Hung, S. P.; Lee, G. H.; Nakano, M.; Tsai, H. L. *Inorg. Chem.* **2010**, *49*, 7617.